

# Measurement of the diffractive structure function $F_2^{D(3)}$

Christophe Royon (for the H1 Collaboration) <sup>a</sup>

<sup>a</sup>Service de Physique des Particules, DAPNIA, CEA-Saclay  
91191 Gif sur Yvette Cedex, France

Measurements of the diffractive structure function  $F_2^{D(3)}(x_P, \beta, Q^2)$ , describing the process  $ep \rightarrow eXY$ , are presented in the two kinematic regions  $0.4 \leq Q^2 \leq 5$ ,  $\text{GeV}^2$ ,  $0.001 \leq \beta \leq 0.65$ , and  $200 \leq \beta \leq 800$   $\text{GeV}^2$ ,  $0.4 \leq \beta \leq 0.9$ , both with  $x_P < 0.05$ ,  $M_Y < 1.6$   $\text{GeV}$  and  $|t| < 1.0$   $\text{GeV}^2$ . Together with published measurements at intermediate  $Q^2$ , the data are compared with models based on QCD and Regge phenomenology. The diffractive trajectory is found to have an intercept larger than that describing soft hadronic data and consistent with that determined using previously published H1 measurements at intermediate  $Q^2$  alone. The data are also parameterised using a QCD motivated model based on the exchange of two gluons from the proton. In this model, the higher twist contribution to  $F_2^{D(3)}$  at large  $\beta$  is found to be important at low  $Q^2$ . The data are also compared with models based on BFKL dynamics.

## 1. Diffractive structure function measurement

In this paper, we report measurements of the diffractive structure function  $F_2^{D(3)}(\beta, Q^2, x_P)$  based on deep-inelastic scattering (DIS) data taken between 1995 and 1997 by the H1 collaboration. The  $F_2^{D(3)}$  measurement describes the process  $ep \rightarrow eXY$ . As in our previous analysis of 1994 data [1], the two distinct hadronic systems  $X$  and  $Y$  are separated by the largest interval in rapidity between final state hadrons. The system  $Y$  is closest to the direction of the outgoing proton beam.

The kinematics of the process can be described by the invariant masses  $M_X$  and  $M_Y$  of the systems  $X$  and  $Y$ , and the Lorentz scalars

$$x = \frac{-q^2}{2P \cdot q} \quad y = \frac{P \cdot q}{P \cdot k} \quad (1)$$

$$Q^2 = -q^2 \quad t = (P - P_Y)^2, \quad (2)$$

where  $P$  and  $k$  are the 4-momenta of the incident proton and electron respectively,  $P_Y$  is the 4-momentum of subsystem  $Y$  and  $q$  is the 4-momentum of the exchanged virtual photon coupling to the electron. The measurements presented here are corrected to the region  $M_Y < 1.6$   $\text{GeV}$  and  $|t| < 1.0$   $\text{GeV}^2$ . The following variables are also defined:

ables are also defined:

$$\beta = \frac{-q^2}{2q \cdot (P - P_Y)} = \frac{Q^2}{Q^2 + M_X^2 - t} \quad (3)$$

$$x_P = \frac{q \cdot (P - P_Y)}{q \cdot P} = \frac{x}{\beta}, \quad (4)$$

where  $W^2 = (q + P)^2$  is the center of mass energy squared of the virtual photon-proton system,  $M_P$  the proton mass and  $x$  is the Bjorken scaling variable.

During the 1994/95 HERA shutdown, the backward region of the H1 detector [2] (the direction of the outgoing electron beam) was upgraded, allowing an extension of the measurement to lower  $Q^2$  and  $\beta$  values compared to 1994 [3]. Using data taken during a period when the interaction vertex was shifted by 70 cm in the proton beam direction, the accessible kinematic range is extended still further. The minimum value of  $Q^2$  at which  $F_2^D$  is measured is thus reduced by a factor 10 and the minimum  $\beta$  by a factor 40 compared to the previous measurement [1].

The good running of the HERA machine in recent years has enabled a large increase in the integrated luminosity recorded by H1. One impact of this increase in statistics is the extension of the accessible kinematic range to higher values of  $Q^2$ . A measurement of  $F_2^{D(3)}$  for  $200 \leq Q^2 \leq 800$   $\text{GeV}^2$  is presented in this paper, based on

positron-proton scattering data collected in the years 1995-1997. This data sample represents an increase in statistics by a factor of around 15 compared to previous H1  $F_2^{D(3)}$  measurements [1].

The structure function  $F_2^{D(3)}$  is calculated from the differential cross section according to the formula

$$F_2^{D(3)} = \frac{\beta^2 Q^4}{4\pi\alpha_{em}^2} \frac{1}{(1-y-\frac{y^2}{2})} \frac{d^3\sigma_{ep \rightarrow eXY}}{dQ^2 d\beta dx}, \quad (5)$$

taking the ratio  $R$  of the longitudinal to the transverse cross sections to be 0.

The high  $Q^2$  data are shown in the form of  $x_P \cdot F_2^{D(3)}$  in figure 1. Due to the kinematic constraints imposed by the large  $Q^2$  values, the measurements are restricted to  $\beta \geq 0.4$  and relatively large  $x_P$ . In Figure 2, the  $Q^2$  and  $\beta$  dependences of the 1994 and low  $Q^2$  1995 measurements of  $F_2^{D(3)}(Q^2, \beta, x_P)$  are shown at a fixed small value of  $x_P$  ( $x_P = 0.005$ ), for which sub-leading exchange contributions are small. We clearly see changes of slopes of scaling violations at low  $Q^2$  ( $Q^2 < 3 \text{ GeV}^2$ ). In the large  $\beta$ , low  $Q^2$  region, additional structures are observed. These are presumably related to higher twist contributions, in particular, the resonant production of vector mesons.

## 2. Interpretation and comparison with models

The results are first used to further constrain the Regge phenomenological model investigated previously [1]. A fit to the combined 1994/1995 points of a single pomeron trajectory with intercept  $\alpha_P(0)$  is not able to describe the data. Addition of a sub-leading (reggeon) trajectory with independent normalisation yields a significantly better description. The intercept trajectories are consistent with the published values [1]. Fits with zero and maximal interference between the two trajectories describe the data equally well. An extension to the fit in which the pomeron intercept takes the form  $\alpha_P(0) = a + b \log Q^2$  gives a value of  $b$  compatible with zero.

The scaling violations of  $F_2^{D(3)}$  as a function of  $Q^2$  motivate an analysis of the data in which

the  $Q^2$  and  $\beta$  dependence of the structure function is understood in terms of parton distribution functions for the pomeron, evolved with perturbative QCD. The quark flavour-singlet and gluon distributions are evolved in  $Q^2$  with the NLO DGLAP equations and fitted, in combination with a reggeon contribution, to the combined data. The extracted parton density functions indicate a large gluonic content (80 – 90%) of the pomeron.

Then we consider the two gluon exchange model for interaction. In a recent paper [5], a parameterization of the diffractive structure function in terms of three main contributions was proposed. The photon fluctuates into partonic states which scatter diffractively. At the beginning of the scattering process, the photon splits into a  $q\bar{q}$  pair, and at sufficient  $M_X^2$ , the  $q\bar{q}$  pair can radiate an additional gluon before it reaches the proton at rest. At small diffractive masses, it is expected that the longitudinal cross section for  $q\bar{q}$  pair production is not small compared to the transverse cross section, this third term appear to be a higher twist contribution. A fit is performed to the combined 1994 and 1995 data with the restriction  $Q^2 > 3 \text{ GeV}^2$  to remain in the domain of perturbative QCD. Two solutions are found (see figure 3) corresponding to large and low  $\gamma$  where  $\gamma$  is a parameter which describes the  $\beta$  dependance of the  $q\bar{q}g$  contribution.

The 1994 and 1995 measurements of  $F_2^{D(3)}$  are also compared with two additional models, the QCD dipole model in which the diffractive interaction is based on BFKL [4] dynamics [6] and the model of Nikolaev et al. [7] (see figure 3). The distinction between these models will be hardly feasible using  $F_2^D$  data alone. Final state and longitudinal structure function measurement may give more hints to distinguish between them.

## REFERENCES

1. H1 Collab., C.Adloff et al., Z. Phys. C76 (1997) 613.
2. H1 Collab., I.Abt et al., Nucl. Instr. and Meth. A386 (1997) 310 and 348.
3. T.Nicholls, PhD Thesis, Univ. of Birmingham, April 1997, M.Dirkmann, PhD Thesis,

- Univ. of Dortmund, 1997, C.Royon, habilitation thesis, University of Orsay, April 1998.
4. V.S.Fadin, E.A.Kuraev, L.N.Lipatov Phys. Lett. B60 (1975) 50.  
I.I.Balitsky, L.N.Lipatov, Sov. J. Nucl. Phys. 28 (1978) 822.
  5. J.Bartels, J.Ellis, H.Kowalski, M.Wuesthoff, preprint DESY 98-034,  
J.Bartels, C.Royon, preprint DESY 98-152
  6. A.Bialas, R.Peschanski, C.Royon, Phys. Rev. D57 (1998) 6899, H.Navelet, R.Peschanski, Ch.Royon, S.Wallon, Phys. Lett. B385 (1996) 357, S.Munier, R.Peschanski, C.Royon, Nucl. Phys. B534 (1998) 297.
  7. M.Bertini et al., Phys. Lett. B422 (1998) 238  
M.Genovese, N.N.Nikolaev, J. Exp. Theor. Phys. 81 (1995) 633.

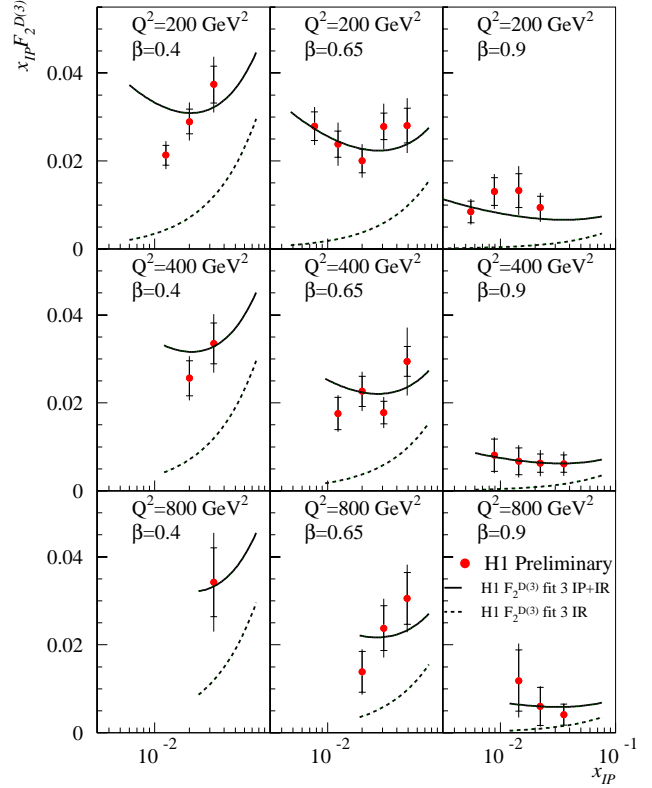


Figure 1.  $x_{IP} \cdot F_2^{D(3)}$  for the large  $Q^2$  measurement, shown as a function of  $x_{IP}$  in bins of  $Q^2$  and  $\beta$ . The inner error bars show statistical errors only. The outer error bars show the statistical and systematic uncertainties added in quadrature. The data are compared to a QCD fit to intermediate  $Q^2$  data with parton distributions for the pomeron and sub-leading exchange evolved into the large  $Q^2$  region using the DGLAP equations.

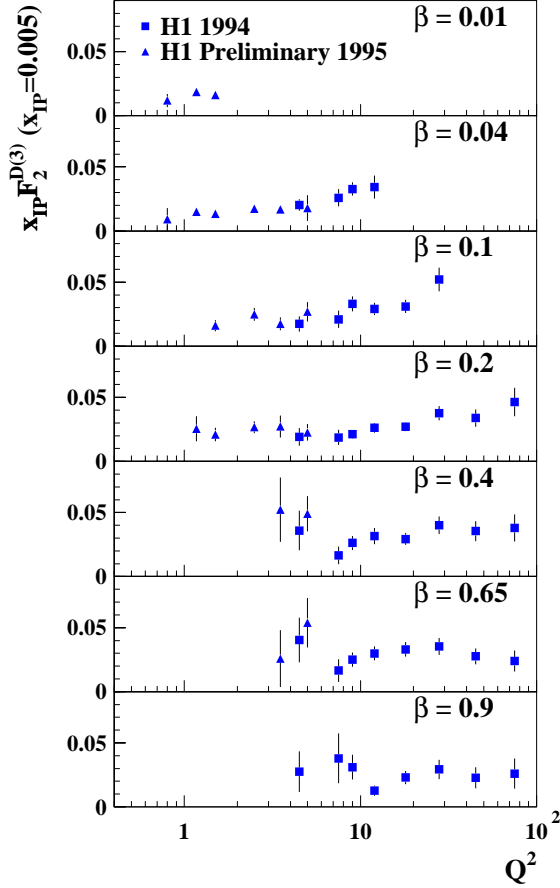


Figure 2. The structure function  $x_{\mathbb{P}} \cdot F_2^{D(3)}$  ( $x_{\mathbb{P}} = 0.005$ ), presented as a function of  $Q^2$  in bins of  $\beta$ , over the full  $Q^2$  range accessed with the 1994 and low  $Q^2$  1995 data sets.

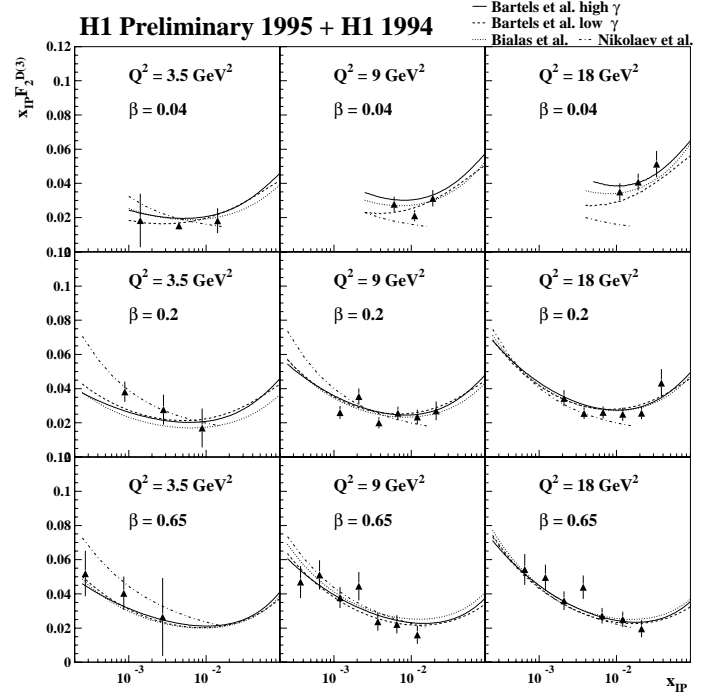


Figure 3. A subset of 1994 and low  $Q^2$  1995 measurements of the structure function  $x_{\mathbb{P}} F_2^{D(3)}$ , showing the  $x_{\mathbb{P}}$  dependence in bins of  $Q^2$  and  $\beta$ . The statistical errors are shown added in quadrature with those systematic errors that vary between data points. Overall normalisation uncertainties of 4.7% for the 1995 data and 6.0% for the 1994 data are not shown. The data are compared to the results of a fit to the Bartels et al. two-gluon exchange model (high  $\gamma$  solution: full line, low  $\gamma$  solution: dashed line), to the fit based on the dipole model of Bialas et al. (dotted line) and to the prediction of the Nikolaev et al. model (dashed-dotted line). For all models except that of Nikolaev et al., an additional sub-leading trajectory is added as described in the text.